

## ARTICLES

**Monte Carlo study of a compressible Ising antiferromagnet on a triangular lattice**

Lei Gu and Bulbul Chakraborty

*The Martin Fisher School of Physics, Brandeis University, Waltham, Massachusetts 02254*

P. L. Garrido,\* Mohan Phani, and J. L. Lebowitz

*Department of Mathematics, Rutgers University, New Brunswick, New Jersey*

(Received 27 July 1995; revised manuscript received 14 December 1995)

We have studied the compressible antiferromagnetic Ising Model on a triangular lattice using Monte Carlo simulations. It is found that the coupling to the strain removes the frustration of the rigid model and the simulations show a transition from the disordered to an ordered, striped phase at low temperatures. This transition involves two broken symmetries: the Ising symmetry and a three-state Potts symmetry characteristic of the triangular lattice. In the absence of bond fluctuations, this transition is always strongly first order. Using finite-size scaling analysis, we find evidence that, in the presence of fluctuations, the transition becomes weakly first order and possibly second order when the coupling to the lattice is increased. We discuss the relevance of this model to certain phase transitions in alloys. [S0163-1829(96)04918-1]

**I. INTRODUCTION**

Frustrated Ising antiferromagnets play an important role in the study of order-disorder transitions in alloys. Many metallic solid solutions form a face-centered-cubic lattice and ordering implies a preference for unlike neighbors which translates into antiferromagnetic interactions in the Ising language. These order-disorder transitions are often accompanied by a *displacive* structural transition where a homogeneous strain transforms the lattice from one form to another.<sup>1</sup> It has been argued, on the basis of theoretical calculations of the stability of metallic alloys,<sup>2-4</sup> that an appropriate model for describing a large class of these alloys is the *compressible* Ising model on a frustrated lattice with some additional terms arising from difference in atomic sizes.<sup>5</sup> This model embodies, in its simplest form, a competition between elastic terms preferring a face-centered-cubic or a triangular lattice and an attractive interaction between unlike atoms which cannot be completely satisfied on such a lattice. Moreover, it is the simplest model which can describe an order-disorder transition accompanied by a displacive structural transition.

In order to understand the basic physics embodied in this model, we have performed simulations on a model two-dimensional system which undergoes a transition from a disordered alloy on a triangular lattice to an ordered alloy on a sheared triangular lattice. This two-dimensional transition corresponds, in three dimensions, to a transformation from a face-centered-cubic to a face-centered-tetragonal lattice. For the sake of simplicity, we have ignored the size-effect term and are, therefore, studying a pure compressible Ising model on a frustrated lattice. The physics of this model is different from the compressible ferromagnetic model since elasticity serves to remove the frustration in this system.<sup>6</sup> It is also different from models of alloys where only size-effect terms are retained.<sup>5</sup>

The elastic antiferromagnet on a triangular lattice has received prior attention. The model has been solved within the magnetothermomechanics approximation in which fluctuations in the bond lengths are neglected.<sup>6</sup> In this approximation, it has been shown that the ground state is a striped phase and there is a single, strong first-order transition from the disordered phase to the striped phase for all parameter values. The transition involves two broken symmetries, the Ising symmetry and a three-state Potts symmetry associated with the directions of bonds on the triangular lattice. The role of bond fluctuations in this model had not been investigated earlier. The appearance of a three-state Potts symmetry in a two-dimensional system raises the question of how these fluctuations affect the nature of the transition and the appearance of two broken symmetries introduces the possibility of two distinct transitions. We have addressed both these questions by including fluctuations of the bonds through Monte Carlo (MC) simulations of the model.

The simulations were carried out on  $L \times L$  triangular lattices with  $L$  ranging from 8 to 64. There are  $N=L^2$  spin variables and  $2N$  continuous variables describing the positions of the atoms. This and the strong first-order transition found for a large range of the parameters, dictated the choice of small system sizes in the interest of obtaining good statistics. We find that the transition is not really different from that observed in Ref. 6. However, the strength of the transition, as deduced from finite-size-scaling analysis, decreases with increasing value of the coupling to the lattice. This is reminiscent of the behavior of the two-dimensional, three-state Potts model, where the fluctuations make the transition second order.<sup>7</sup> In the absence of any exact results in our model, more extensive simulations are needed to make a definitive statement about whether or not there is a critical coupling at which the transition becomes second order. The simulations show no evidence for two distinct transitions.

The contents of the paper are organized as follows: the Hamiltonian for the compressible triangular Ising lattice and the ground states of this model are discussed in Sec. II; the algorithm for the Monte Carlo simulation including spins and lattice displacements is given in Sec. III; general features of the simulations are presented in Sec. IV and the finite-size scaling analysis performed to assess the strength of the transition is presented in Sec. V. A discussion of open problems is presented in Sec. VI.

## II. THE MODEL

The compressible Ising model involves two sets of variables, the spins  $s(m,n) = \pm 1$  and the displacements  $\mathbf{u}(m,n)$  which define the displacement of the spin from the original lattice site  $(m,n)$ . On a triangular lattice, the positions of the spins on the undistorted lattice are defined by  $\mathbf{r}^0(m,n) = m\mathbf{a}_1 + n\mathbf{a}_2$  with  $\mathbf{a}_1 = (1,0)$  and  $\mathbf{a}_2 = (1/2, \sqrt{3}/2)$ . The actual positions of the spins are, therefore, given by  $\mathbf{r}(m,n) = \mathbf{r}^0(m,n) + \mathbf{u}(m,n)$ . The interaction between the spins depends on the *distance* between them and, in our model as in usual compressible Ising models,<sup>6</sup> a linear dependence is assumed:

$$J(mn; m'n') = J^0(mn; m'n') \times \{1 - \epsilon[|\mathbf{r}(m,n) - \mathbf{r}(m',n')| - 1]\}. \quad (1)$$

Here  $\epsilon$  defines the strength of the coupling between the spins and the displacements and the bare spin-spin interaction is given by  $J^0$ . For the nearest-neighbor antiferromagnet, we take  $J^0 = 1$  for nearest neighbors and zero otherwise. All energies are therefore measured in units of the nearest-neighbor spin interaction. The value of  $\epsilon$  is chosen to be positive which ensures that the antiferromagnetic interaction gets stronger as the spins get closer to each other.

Besides the spin-spin interaction, the Hamiltonian involves a harmonic lattice Hamiltonian defining the deformability of the lattice: a quadratic form in the displacements which involves the dynamical matrix.<sup>8</sup> If the displacements vary slowly over length scales comparable to the lattice spacing, a coarse-grained form of this Hamiltonian, written in terms of the strain fields is appropriate.<sup>8</sup> We use this coarse-grained form in our model. Choosing the nearest-neighbor directions to express the strain tensor,<sup>6</sup> the elastic Hamiltonian can then be written as

$$H_{\text{el}} = \sum_{\alpha\beta} \sum_{m,n} D_{\alpha\beta} e_{\alpha}(m,n) e_{\beta}(m,n). \quad (2)$$

Here the strain tensor components  $\{e_{\alpha}, \alpha = 1, 2, 3\}$  are related by a linear transformation to the usual Cartesian components  $\epsilon_{xx}$ ,  $\epsilon_{xy}$ , and  $\epsilon_{yy}$ , and this transformation defines  $D_{\alpha\beta}$  in terms of the elastic constants:

$$D = 1/2 * \begin{pmatrix} E & \Lambda & \Lambda \\ \Lambda & E & \Lambda \\ \Lambda & \Lambda & E \end{pmatrix}. \quad (3)$$

The constants  $E$  and  $\Lambda$  are related to the Young's modulus  $Y$  and Poisson ratio  $\sigma$ :<sup>6</sup>

$$Y = E(2 - \Lambda)(1 + \Lambda)/(2 + \Lambda), \quad (4)$$

$$\sigma = (2 + 5\Lambda)/3(2 + \Lambda). \quad (5)$$

The strain fields  $e_{\alpha}(m,n)$  are related to the displacement  $\mathbf{u}(m,n)$  through the relation

$$e_{\alpha}(m,n) = \frac{[\mathbf{u}(m',n') - \mathbf{u}(m,n)]_{\alpha} [\mathbf{r}_0(m',n') - \mathbf{r}_0(m,n)]_{\alpha}}{|\mathbf{r}^0(m',n') - \mathbf{r}^0(m,n)|^2}. \quad (6)$$

We choose our length scale such that  $|\mathbf{r}^0(m',n') - \mathbf{r}^0(m,n)|^2 = 1$ .

For displacements with amplitudes much smaller than 1,

$$e_{\alpha}(m,n) \approx |\mathbf{r}(m',n') - \mathbf{r}(m,n)|_{\alpha} - 1 \equiv \nu_{\alpha}(m,n), \quad (7)$$

where  $\mathbf{r}(m',n')$  and  $\mathbf{r}(m,n)$  are positions of nearest-neighbor spins along the  $\alpha$  direction. The total Hamiltonian can then be written as

$$H = \sum_{\alpha} \sum_{m,n} [1 - \epsilon \nu_{\alpha}(m,n)] \Theta_{\alpha}(m,n) + \sum_{\alpha\beta} \sum_{m,n} D_{\alpha\beta} \nu_{\alpha}(m,n) \nu_{\beta}(m,n). \quad (8)$$

Here  $\Theta_{\alpha}(m,n) = s(m,n)s(m',n')$  and  $s(m,n)$  and  $s(m',n')$  are nearest neighbor spins along  $\alpha$  direction. In our simulations, we use Eq. (8) and therefore, assume that the strain field is approximated well by Eq. (7).

The coarse-grained elastic Hamiltonian, expressed in Eqs. (1) and (7), is the natural and most convenient form to use in investigating the effect of strain fluctuations on the phase transition to the striped phase, studied by Chen and Kardar<sup>6</sup> within the mean-field approximation. In this approximation, the spins are treated exactly but the strain fields are uniform:  $e_{\alpha}(m,n) = e_{\alpha}$ . The coarse-grained form is valid only when the displacement fields vary slowly over the length scale of the lattice<sup>8</sup> and by adopting this form, we are restricting ourselves to this class of displacements. The alternative would be to allow arbitrary displacements and work with the more microscopic Hamiltonian defined in terms of the displacements. The two approaches are equivalent as long as long-wavelength fluctuations play the dominant role in the phase transition.

### Ground states of model

The nature of the antiferromagnetic Ising model on the triangular lattice is well known from the work of Wannier.<sup>9</sup> There is no long-range order because of the degeneracy of the ground state and the  $T=0$  state is a critical state with power-law correlations.<sup>10</sup> Chen and Kardar<sup>6</sup> have shown that the introduction of elasticity in the magnetothermomechanics approximation where all  $e_{\alpha}(m,n) = e_{\alpha}$ , removes the degeneracy of the ground state, and at low temperature, the system orders into a striped phase consisting of alternating rows of spin up and spin down and a distorted lattice with the  $(++)$  and  $(--)$  bonds longer than the  $(+-)$  bonds. The striped phases are the only ground states of the model defined by Eqs. (1) if one imposes the condition of slow variation of displacement fields, implicit in the definition of the

coarse-grained elastic Hamiltonian. An interesting aspect of this model is that if no constraints are imposed, the model defined by Eq. (1) has an infinite number of new ground states whose logarithm grows with the linear dimensions of the system and which do not have a Bravais lattice structure.<sup>11</sup> These ground states are obtained from joining together minimal triangles which are triangles that have two short (+ -) bonds and one long (+ +) or (- -) bond. The model can then still be frustrated, at least in two dimensions. However, the displacements required to reach these ground states vary on the same scale as the lattice spacing and the approximations leading to the coarse-grained, strain-field Hamiltonian [Eq. (8)] are not valid. To compare the energetics of these states with the striped phases, one has to go back to the elastic Hamiltonian written in terms of the displacement fields.<sup>8</sup> By doing so, we can show that these new ground states are higher in energy than the striped phase with the cost in energy increasing as  $\approx[\epsilon/(E+\Lambda)]^2$ . Therefore, we do not believe these ground states are physically realizable. In our simulations, the constraint of slow variation is explicitly imposed.

The striped phase can have the expanded bonds oriented along one of the three nearest-neighbor directions on the triangular lattice. Therefore, a continuous-spin, three-state Potts variable can be associated with each of the triangles on the lattice with the Potts variables located at the center of the triangles and the Ising variables located at the vertices. At the transition from the disordered to the striped phase, two symmetries are broken: the Ising symmetry and the three-state Potts symmetry. It is well known that in the two-dimensional, three-state Potts model, fluctuations change the order of the transition from first to second. One of the interesting questions that can be addressed in our simulations is, therefore, whether bond fluctuations convert the strongly first-order transition to the striped phase<sup>6</sup> into a second-order transition.

The lattice distortion in the ground state can be easily calculated and is described by a homogeneous strain deformation defined by

$$e_1 = \frac{\epsilon(E+3\Lambda)}{(E+2\Lambda)(E-\Lambda)}, \quad (9)$$

$$e_2 = e_3 = \frac{-\epsilon(E+\Lambda)}{(E+2\Lambda)(E-\Lambda)}. \quad (10)$$

The spin structure in the ground state is such that the spins are aligned parallel to each other in the direction along which the bonds are stretched and aligned antiparallel to each other in the other two directions.

In this paper, we specialize to the case where  $\Lambda=0$ . According to Eqs. (3) and (4), this implies that the Young's modulus is identical to  $E$  and the Poisson ratio is  $\sigma=1/3$ . This is not a special point in the parameter space of this model and the mean-field phase diagrams of Ref. 6 demonstrate that this point has a generic phase diagram. The corresponding ground state deformations are given by  $e_1 = \epsilon/E$  and  $e_2 = e_3 = -\epsilon/E$ . The ground state energy (per unit bond) is then

$$E^0(\epsilon, E) = -\frac{1}{3} - \frac{\mu}{2}. \quad (11)$$

The parameter,  $\mu = \epsilon^2/E$  appearing in this equation is the effective coupling constant of our mode.<sup>6</sup> It is seen clearly that the interaction with the lattice reduces the energy of the striped phase compared to a rigid antiferromagnet and makes it stable under small perturbations. The stability of the striped phase increases with increasing  $\mu$ . In our simulations, this is reflected in the transition temperature increasing with increasing values of  $\mu$ . At  $\mu \geq 1$ , the distortion of the lattice in the ground state is such that the spin-spin interaction along the expanded bond ( $e_1$ ) changes sign and is ferromagnetic for larger values of  $\mu$ . This is an example of the effectiveness of the lattice distortions in removing frustration.

From an investigation of the stability of the ground state, it is clear that the triangular lattice collapses to a line for  $\epsilon/E \geq 1/3$ . The parameter range considered in the simulations was restricted to the region where the triangular lattice is stable.

Since the striped phase is threefold degenerate corresponding to the three possible directions of spin ordering on the triangular lattice, we have to introduce three order parameters to describe the ordering along each of the three directions. They are defined as follows:

$$\Psi[1] = \sum_{m,n} (-)^m s(m,n), \quad (12)$$

$$\Psi[2] = \sum_{m,n} (-)^n s(m,n), \quad (13)$$

$$\Psi[3] = \sum_{m,n} (-)^{m+n} s(m,n). \quad (14)$$

In addition, we need to define the strain order parameters:  $e_\alpha = (1/N) \sum_{m,n} e_\alpha(m,n)$  which also acquire a nonzero value in the striped phase. There are three components of the energy: the spin-spin energy  $E_s$  determined by the nearest-neighbor spin-spin correlation functions  $\langle s(m,n)s(m',n') \rangle$ ; the spin-lattice energy,  $E_{s,l}$ , determined by the spin-strain correlation functions  $\langle \Theta_\alpha(m,n)e_\alpha(m,n) \rangle$  and the lattice energy,  $E_{el}$ , determined by the strain-strain correlation functions  $\langle e_\alpha(m,n)e_\beta(m,n) \rangle$ . The distribution of these energies is monitored in order to investigate the nature of the transition to the striped phase.

### III. SIMULATION METHOD

We are interested in simulating the model defined by Eq. (1) which has two sets of variables, the discrete Ising spins and the continuous strain fields. We define the strain fields in terms of the distance between two spins using Eq. (6). The distances are changed by allowing displacements  $\mathbf{u}(m,n)$  at each site. The displacements  $\mathbf{u}(m,n)$  as well as the spins  $s(m,n)$  are subjected to periodic boundary conditions. This implies that the homogeneous strain deformations have to be treated separately. Therefore, besides the spin and displacement variables, the simulations have to allow for changes in the shape and the size of the simulation box.

As discussed in Sec. II, the displacements,  $\mathbf{u}(m,n)$ , which define the fluctuations of the strain fields, have to be slowly varying to justify the coarse-grained Hamiltonian. One way to impose this constraint would be to deal exclusively with long-wavelength distortions by working in Fourier space. We choose to work in real space and impose a constraint on the amplitude of the displacements to indirectly guarantee a slow variation on the length scale of the lattice. It should be emphasized that the amplitude of the homogeneous strain fields are not restricted, only the amplitude of the fluctuations are. By adopting this procedure, we study the effects of long-wavelength small ( $\ll 1$ ) amplitude fluctuations on the transition to the striped phase.

One MC step consists of two parts. The first part involves changing the shape and volume of the box. This is done once per MC step. This MC move is similar to the one used by Dünweg and Landau,<sup>5</sup> in their work on the size-effect model, where the volume of the lattice was allowed to change. The only difference between the two algorithms is that we do not rescale the position of each individual spin after we change the shape and volume of the lattice and, therefore, our simulations do not involve the additional logarithmic term in the effective energy [cf. Eq. (2.14) in Dünweg and Landau].<sup>5</sup> This rescaling would have involved a more complicated function in the presence of the shape changes that are allowed in our simulations.

In Monte Carlo simulations<sup>12</sup> involving continuous variables, it is necessary to choose an amplitude which defines by how much the continuous variable is changed in a Metropolis trial. The shape and volume of the box are changed by allowing changes in the lattice parameters and the angle between the lattice vectors  $\mathbf{a}_1$  and  $\mathbf{a}_2$ . The amplitude for each of these changes is normally a very small number, of the order of 0.01, and is chosen by requiring a Monte Carlo acceptance rate of 50–60%.

The second part of the MC involves updating the spins and displacements at each node  $(m,n)$  of the newly defined lattice, with updated  $\mathbf{a}_1$  and  $\mathbf{a}_2$ , and involves  $N$  trials where  $N$  is the number of spins. Each trial is composed of one attempt to flip a spin and one attempt to change the position of the spin. To update the position of a spin, keeping in mind the constraint of slow variations of displacements, we choose a random position inside a circle of radius  $u_{\max}$  centered on an updated lattice site. This sets an upper limit on the amplitude of the displacements. Choosing  $u_{\max} \approx \epsilon/E$ , guarantees that the variation in displacements over one lattice constant is at most twice the ground state distortion. It also ensures that the displacements do not lead to exchanges of sites which would certainly violate the assumption of slowly varying fields.

#### IV. GENERAL RESULTS FROM THE SIMULATIONS

We have carried out Monte Carlo simulations for different values of the parameter  $\mu$  which measures the coupling to the lattice. The ratio  $\epsilon/E$  was held constant at 0.3. This ensures that the ground state distortion remains the same as  $\mu$  is varied, and allows us to monitor the changes in the transition between exactly the same two states.

For each value of  $\mu$ , two sets of simulations were performed, one allowing only global changes of the lattice pa-

TABLE I. Theoretical predictions for  $T_c^L$  compared to our simulation results (with and without local bond fluctuations). The theoretical results are those of Ref. 6 obtained within the magnetothermomechanics approximation which neglects fluctuations of the strain fields.

$\mu = \epsilon^2/E$	$1/T_c$ (Theory)	$1/T_c^L$ (No fluctuations)	$1/T_c^L$ (With fluctuations)	Size
0.18	1.5	1.5-1.52	1.56	$64 \times 64$
0.18	1.5	1.35	1.45	$10 \times 10$
3.0	0.14	0.16	0.20	$22 \times 22$
6.0	0.09	0.09	0.13	$22 \times 22$
10.0			0.08	$22 \times 22$

rameters, corresponding to a homogeneous strain deformation, and the other including bond fluctuations according to the algorithm described earlier.

The results of Chen and Kardar<sup>6</sup> are exact in the limit of no bond fluctuations and our simulation results from finite-sized systems are compared to their exact results in Table I. For  $\mu = 0.18$ , two sets of results are quoted, one for a system of size  $10 \times 10$  and the other for a system of size  $64 \times 64$ . As expected, the transition temperature is reduced upon introduction of bond fluctuations. One also observes a trend of increasing effects of fluctuations on  $T_c^L$ , the transition temperature for system size  $L$ , as the coupling  $\mu$  is increased. For example, the relative change in  $T_c^L$ , upon introduction of bond fluctuations, is only 3% for  $\mu = 0.18$ , whereas the relative change is close to 50% for  $\mu = 6.0$ . In these simulations, we also observe a change in the nature of the transition as  $\mu$  is varied. The fluctuations in bond lengths are much more prominent for larger values of  $\mu$ . We have found no evidence for the existence of an intermediate state leading to two distinct transitions.

The phase diagrams obtained from the simulations with and without bond fluctuations are compared in Fig. 1. This

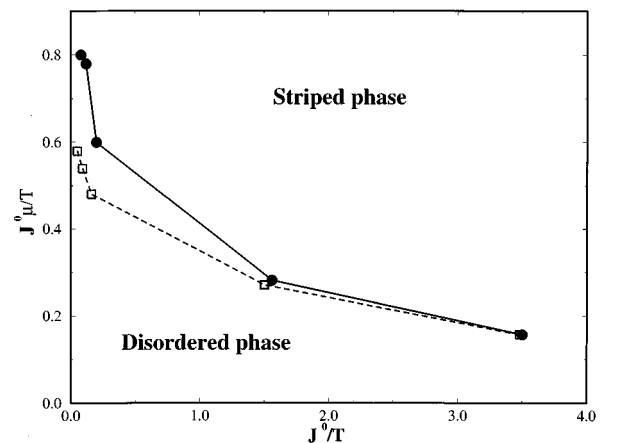


FIG. 1. Phase diagrams obtained from our computer simulations, which should be compared to the phase diagram in Ref. 6 for  $\Lambda = 0$ . Solid line (filled circle symbol) is obtained with strain fluctuations. Dashed line (open square symbol) is obtained without strain fluctuations. The solid and dashed lines are plotted here to guide the eyes.

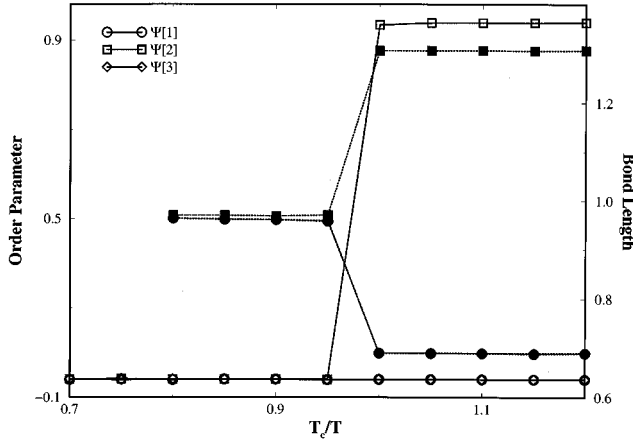


FIG. 2. The three spin order parameters,  $\Psi[1]$ ,  $\Psi[2]$ , and  $\Psi[3]$ , plotted as a function of  $T_c^L/T$  for  $\mu=3.0$  for system size  $22 \times 22$ . The circles and diamonds refer to the two nonordering directions while squares refer to the ordering one. This plot is overlaid with the plot of the three average bond lengths which are determined by the strain order parameters,  $e_\alpha = (1/N) \sum_{(m,n)} e_\alpha(m,n)$ . Filled circles and diamonds refer to the contracted bonds, while filled squares refer to the expanded bond. This figure clearly shows that the transition is to the striped phase where the spin ordering is accompanied by a structural distortion.

figure demonstrates the effects of bond fluctuations on the phase boundary. It is clear that, in accordance with our expectations, fluctuations depress the transition temperature. If there is a change in the nature of the transition, caused by the fluctuations, it cannot be deduced from a perusal of the phase diagram and we have performed finite-size scaling analysis to pursue this question.

The phase transition in this model is an example of a spin ordering accompanied by a structural transition and, before discussing the finite-size scaling analysis, we would like to point out some generic features of the transition using the results from simulations at  $\mu=0.18$ , one of the smallest values of  $\mu$  that we have studied.

The transition is characterized by the appearance of a nonzero spin order parameter [Eqs. (15)–(17)] and strain order parameters defined by  $e_\alpha = (1/N) \sum_{m,n} e_\alpha(m,n)$ . The nonzero strain order parameters lead to a change in the bond lengths and, Fig. 2 shows the variation of the spin order parameters and the bond lengths as a function of temperature. This figure demonstrates that there is a single transition at which both the Ising and Potts symmetries are broken and the ordered state is the striped phase where the bonds between parallel spins are elongated and bonds between antiparallel spins are contracted.

In Fig. 3, we show averages of the various components of the energy and compare them to the results of simulations with no bond fluctuations. The effect of the fluctuations in reducing the transition temperature is obvious. Deducing the strength of a transition from plots of order parameters or energy is often risky and we will defer that discussion to our finite-size scaling analysis. One interesting aspect of these results is that there is a difference in the elastic energy and spin-lattice energy between the fluctuating and the nonfluctuating case. This difference is attributed to the local bond

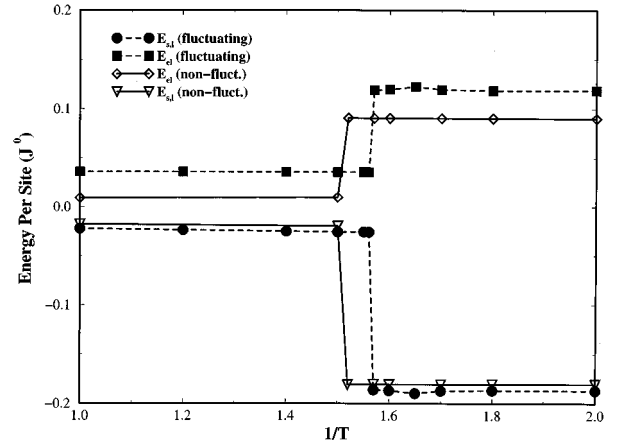


FIG. 3. The spin-lattice ( $E_{s,l}$ ) and the pure lattice ( $E_{el}$ ) contributions to the energy are shown as a function of  $1/T$  for  $\mu=0.18$  and system size  $64 \times 64$ . The energy is measured in  $J^0$ , the bare spin-spin antiferromagnetic interaction. The open triangles and diamonds (connected by dashed line) refer to the nonfluctuating case, while filled square and circles (solid line) to the fluctuating case. The spin-lattice energy,  $E_{s,l}$  is given by the triangles (nonfluctuating) and circles (fluctuating), while  $E_{el}$  is given by the diamonds (non-fluctuation) and squares (fluctuating).

fluctuations and can be understood by making a simple harmonic model for each atom fluctuating within the the circle of radius  $u_{\max}$  (cf. Sec. III).

For  $\mu=0.18$ , the smallest value considered by us, we found that to obtain accurate statistics in systems as large as  $64 \times 64$ , the MC runs have to be extremely long. In the current simulation for size  $64 \times 64$ , which were run for approximately by 500 000 steps, the distribution does not reach a stable double-Gaussian structure indicating that the tunneling times, between two coexisting states, are comparable to the total time of a run. This indicates pronounced metastability or a strong first-order transition. By comparing to simulations on much smaller systems, for example  $8 \times 8$ , we find that the results are consistent with tunneling times scaling exponentially with system size which is characteristic of a first-order transition in a standard canonical simulation.<sup>13</sup>

## V. CHANGES WITH CHANGING $\mu$

The results presented in the previous section indicate that the transition remains strongly first order, in the presence of fluctuations, for small values of  $\mu$ . Therefore, our model does not behave like the three-state Potts model in spite of the bond order parameters exhibiting this symmetry. An interesting question to ask is whether this behavior gets modified by increased coupling to the lattice. In the rest of the paper, we present results which show the transition becomes weaker as the coupling to the lattice is increased.

As we increased  $\mu$ , we observed higher transition temperatures, lower activation barriers and shorter tunneling times between coexisting states. For example, for  $\mu$  larger than 3.0, it was much easier to get the system to order into the striped phase in a cooling run. Also, there were no noticeable hysteresis effects in system sizes of the order of  $22 \times 22$  if the simulations involve 10,000 to 20,000 steps. This

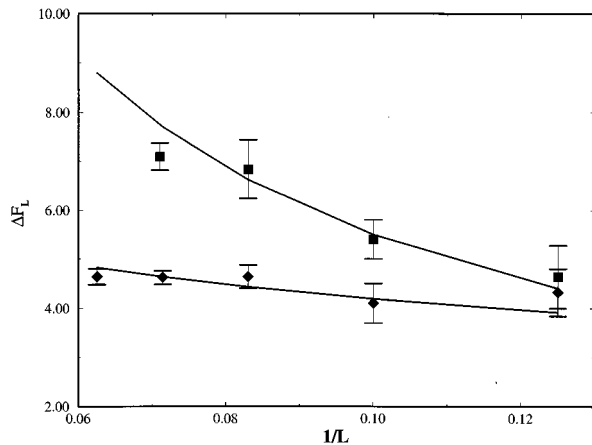


FIG. 4. Plot of  $\Delta F(L)$  versus  $1/L$  for  $\mu=3.0$  (filled square symbol) and for  $\mu=6.0$  (filled diamond symbol). For a first-order transition,  $\Delta F(L)$  should increase monotonically with  $L$  and be proportional to  $L$  in the strong first-order regime (cf. text for discussion). We have fitted the data for  $\mu=3.0$  to a straight line  $0.55 * L$ , while fitting the data for  $\mu=6.0$  to  $2.1 * L^{0.3}$ , which indicates a weak first-order transition.

is in sharp contrast to the  $\mu=0.18$  simulations. For larger values of  $\mu$ , the transition appeared continuous in the system sizes looked at (largest size being  $26 \times 26$ ) and we observed large fluctuations in the energy and order parameters near  $T_c^L$ .

The qualitative picture suggested by these observations is that the interfacial free-energy decreases as the coupling to the lattice is increased leading to weaker first-order transitions. This is reminiscent of the changes observed in the Potts model, and we have performed finite-size scaling analysis in order to determine the strength of the transitions.

#### Finite size scaling analysis

The finite-size scaling analysis<sup>14</sup> was restricted to fairly small systems, sizes ranging from  $8 \times 8$  to  $26 \times 26$ , in the interest of obtaining good statistics.<sup>7, 15, 16</sup> For  $\mu=0.18$ , we also have results from  $64 \times 64$ .

In order to assess the strength of the first-order transitions, we adopted the Lee-Kosterlitz approach.<sup>7, 17</sup> This approach is based on analyzing the probability distribution of energy,  $P(E)$ , and studying the scaling behavior of  $\Delta F(L)$ , the free-energy barrier between coexisting states. According to their analysis,  $\Delta F(L)$  increasing with the system size signals a first-order transition. A constant  $\Delta F(L)$  is characteristic of a critical point and a decreasing behavior indicates a disordered phase. Moreover, if  $\Delta F(L) \gg 1$ , then the system is in the regime where leading order finite-size corrections are applicable, and  $\Delta F(L)$  grows as  $L^{d-1}$ .

Our model is interesting from the point of view of first-order phase transitions for a couple of reasons. One is that it involves two coupled degrees of freedom, the spins and the strain fields, and the other is that in the limit of zero coupling the system is completely frustrated. The Lee-Kosterlitz approach,<sup>7</sup> described in the context of the  $\mu=0.18$  simulations, is based upon very general ideas and should be valid for any system where there is a clearly defined interface between the two coexisting states at a first-order transition.

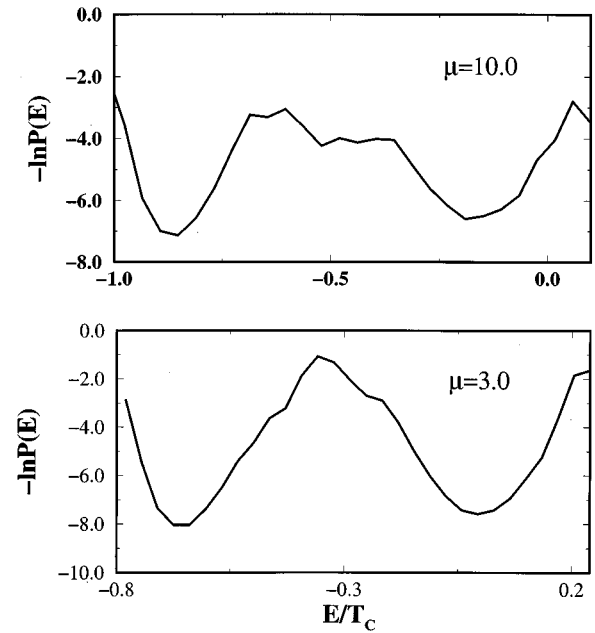


FIG. 5. The negative of the logarithm of the probability distribution of energy,  $-\ln P(E)$  at  $T_c^L$ , for system size  $10 \times 10$  for  $\mu=3.0$  and  $\mu=10.0$ . The distribution for  $\mu=3.0$  can be well described by a double Gaussian and  $\Delta F(L)$ , the activation energy measured by the difference between the maximum and the minima in the figure, is seen to be much larger than 1.0. In contrast, the distribution for  $\mu=10.0$  has a pronounced non-Gaussian structure and  $\Delta F(L)$  is of the order of 1.

In Fig. 4, we compare the scaling behavior of  $\Delta F(L)$  for  $\mu=3.0$  and  $\mu=6.0$ . We find that  $\Delta F(L)$  scales as  $L$  for  $\mu=3.0$  but for  $\mu=6.0$ ,  $\Delta F(L)$  increases much more slowly. This is indicative of a weakening transition.<sup>7, 17</sup> Comparing these plots with the results of Lee and Kosterlitz<sup>17</sup> for  $Q$ -state Potts model at  $Q=8$  and  $Q=5$ , we see a striking similarity between the plots for  $\mu=3.0$  and  $Q=8$  and the plots for  $\mu=6.0$  and  $Q=5$ . This raises the possibility of a crossover to a second-order transition, since in the Potts model the transition does become second order at  $Q=4$ .

Figure 5 compares the negative of the logarithm of the probability distribution of energy,  $-\ln P(E)$  [from which  $\Delta F(L)$  is obtained], for a system of size  $10 \times 10$  for  $\mu=3.0$  and  $\mu=10.0$ . In contrast to the distribution for  $\mu=3.0$ , which can be described very well by a double Gaussian, the distribution for  $\mu=10.0$  has a pronounced non-Gaussian structure.  $\Delta F(L)$ , as measured by the difference between the maximum and the minima in Fig. 5, is  $\approx 5$  for  $\mu=3.0$ , whereas it is hard to define and smaller for  $\mu=10.0$ . The trends in the probability distributions are consistent with the trends observed in the scaling of  $\Delta F(L)$ . When we repeated the simulations for  $\mu=3.0$  with a system of size  $6 \times 6$ , the double Gaussian distribution changed and the system exhibited pseudocritical behavior. This is similar to the observations made by Peczak and Landau in the two-dimensional Potts model<sup>15</sup> when the system size was comparable to or less than the correlation length.

In contrast to the simulations discussed here, the global simulations do not change their character significantly as  $\mu$  varies and the nature of transition remains strongly first-

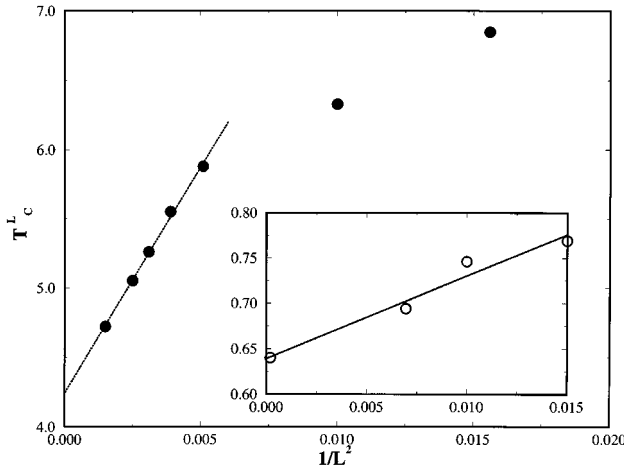


FIG. 6. Plot of  $T_c^L$  as a function of  $1/L^2$  for  $\mu=3.0$  (filled circles) and for  $\mu=0.18$  (open circles). For  $\mu=3.0$ , the data for  $L>16$  can be fitted to a straight line (dashed line in the figure) in accordance with the predictions of finite-size scaling. For  $\mu=0.18$ , the data can be fit by a straight line over the complete range of system sizes from  $L=8$  to  $L=64$  (solid line in the inset). The extrapolated values of  $T_c$  for an infinite system are 0.639 for  $\mu=0.18$  and 4.24 for  $\mu=3.0$ .

order, in agreement with the exact results in this limit.<sup>6</sup> The change in the nature of the transition is therefore, a pure bond fluctuations effect.

Based upon the size and scaling of  $\Delta F(L)$ , we expect the  $\mu=0.18$  and  $\mu=3.0$  simulations to follow the standard finite-size scaling predictions for thermodynamic quantities. The finite-size scaling prediction for  $T_c^L$  is that its deviation from the infinite-system  $T_c$  should scale as  $L^{-d}$  where  $d$  is the spatial dimension.<sup>13</sup> Figure 6 shows  $T_c^L$  as a function of  $L^{-2}$ . For  $\mu=3.0$ . The behavior is linear with a crossover observed at  $L=16$ . For  $\mu=0.18$ , the finite-size scaling predictions are obeyed over the full range of system sizes from  $8 \times 8$  to  $64 \times 64$ .

One interesting difference between our model and the Potts model is the existence of two coupled degrees of freedom, the spins and the strain fields, and the concomitant appearance of two broken symmetries. The physics behind the weakening transition can, therefore, be very different. Investigation of the probability distributions of the individual contributions to the energy can provide us with information relevant to this point. Comparing the changes in these distributions as  $\mu$  increases, we find that the width of  $P(E_{\text{tot}})$ , the distribution of the total energy, increases and it starts to resemble the distribution for the lattice energy,  $P(E_{\text{el}})$ . The width of  $P(E_{s,l}+E_s)$  remains narrow. We believe that as we increase  $\mu$ , the contribution of  $E_{\text{el}}$  to  $E_{\text{tot}}$  becomes more and more important, causing bond fluctuations to play a much larger role in total energy distribution, and the fluctuations in the Potts variables leads to a weakening of the transition. Another interesting aspect of these simulations is that although the transition weakens as  $\mu$  is increased, the spin-

spin part of the energy shows a larger discontinuity as  $\mu$  is increased. This is in contrast to pure spin model where a weakening transition would imply a smaller latent heat which means a smaller discontinuity in the spin energy. In our model, the latent heat does decrease but the spin-spin contribution to it increases.

## VI. CONCLUSIONS

In this paper, we have studied a simple model of an order-disorder transition accompanied by a displacive structural transition. Just as the Ising model provided a framework for studying the statistical mechanics of ordering in alloys, this, extended Ising model, provides a general framework for describing phase transitions in alloys where the ordering is accompanied by a displacive structural change.

Our simulations have shown that fluctuations of the strain field lead to changes in the nature of the phase transition as the coupling between the strain field and the ordering (concentration) field is increased. The transition evolves from being strongly first order to weakly first order. This could lead to interesting, observable pretransitional effects in alloys whose real materials parameters place them in the weak first-order regime. We have extracted the parameters relevant to CuAu from calculations based on a microscopic Hamiltonian<sup>18</sup> and found  $\mu=4.0$ , placing CuAu close to the strongly first-order category; consistent with experiments.<sup>1</sup> Fluctuations in three dimensions can be qualitatively different from two-dimensional models and this needs to be investigated further. However, since the geometric frustration in the face-centered-cubic lattice is of the same nature as that in the triangular lattice, we can hope to describe real alloys by using real materials parameters in the two-dimensional model.

One of the most fascinating aspects of alloy physics is the nature of metastable and unstable states and the kinetics of nucleation and growth. The study of the kinetics of our model should lead to a better understanding of these phenomena in the presence of homogeneous strain fields of the type associated with displacive phase transitions. Martensites undergo displacive phase transitions which do not necessarily involve an configurational order-disorder transition and there have been extensive studies of these systems.<sup>19</sup> An interesting aspect of our model is the fundamental role of the coupling between the strain field and the ordering field: in the absence of the coupling, there is no displacive phase transition.

## ACKNOWLEDGMENTS

We would like to acknowledge useful discussions with A. Mazel, W. Klein, Duane Johnson, N. Gross, and H. Gould. The work of L.G. and B.C. was supported in part by DE-FG02-ER45495. The work of P.L.G., M.P., and J.L.L. was supported by NSF through DMR. The work of P.L.G. was also supported by DGICYT (PB91-0709) and Junta de Andalucía (PAI) of Spain.

- \*Permanent address: Instituto Carlos I de Física Teórica y Computacional, Facultad de Ciencias, Universidad de Granada, E-18071 Granada, Spain.
- <sup>1</sup>W. B. Pearson, *Handbook of Lattice Spacings and Structures of Metals* (Pergamon, New York, 1958).
- <sup>2</sup>Zhigang Xi *et al.*, J. Phys. Condens. Matter **4**, 7191 (1992).
- <sup>3</sup>Bulbul Chakraborty, in *Metallic Alloys: Experimental and Theoretical Perspectives*, edited by J. S. Faulkner and R. G. Jordan (Kluwer Academic, Netherlands, 1994).
- <sup>4</sup>B. Chakraborty, Europhys. Lett. **30**, 531 (1995).
- <sup>5</sup>B. Dünweg and D. P. Landau, Phys. Rev. B **48**, 14 182 (1993); P. Fratzl and O. Penrose, Acta. Metall. Mater. **43**, 2921 (1995).
- <sup>6</sup>Z. Y. Chen and M. Kardar, J. Phys. C **19**, 6825 (1986).
- <sup>7</sup>J. Lee and J. M. Kosterlitz, Phys. Rev. B **43**, 3265 (1991) and references therein.
- <sup>8</sup>cf. N. W. Ashcroft and N. D. Mermin, *Solid State Physics* (Holt, Rinehart, and Winston, New York, 1976), Chap. 22.
- <sup>9</sup>G. H. Wannier, Phys. Rev. **79**, 357 (1950).
- <sup>10</sup>O. Nagai *et al.*, Phys. Rev. B **47**, 202 (1991); John Stephenson, J. Math. Phys. **11**, 413 (1970).
- <sup>11</sup>Alik Mazel (private communication).
- <sup>12</sup>K. Binder and D. W. Heermann, *Monte Carlo Simulation in Statistical Physics* (Springer-Verlag, Berlin, 1988).
- <sup>13</sup>Bernd A. Berg and Thomas Neuhaus, Phys. Rev. Lett. **68**, 9 (1992).
- <sup>14</sup>M. S. S. Challa, D. P. Landau, and K. Binder, Phys. Rev. B **34**, 1841 (1986).
- <sup>15</sup>P. Peczak and D. P. Landau, Phys. Rev. B **39**, 11 932 (1989).
- <sup>16</sup>C. Borgs *et al.*, J. Phys. (France) I **4**, 1027 (1994).
- <sup>17</sup>J. Lee and J. M. Kosterlitz, Phys. Rev. Lett. **65**, 137 (1990).
- <sup>18</sup>The parameters appropriate for CuAu were calculated by fitting the ground-state energy calculated from the microscopic model described in Ref. 2 to the model used in this paper.
- <sup>19</sup>*Martensite*, edited by G. B. Olson and W. S. Owen (ASM International, Metals Park, OH, 1992); Phys. Rev. B **39**, 11 932 (1989).